ARCHIVES OF ELECTRICAL ENGINEERING VOL. 60(3), pp. 223-230 (2011)

DOI 10.2478/v10171-011-0021-8

Measurement and calculation of 3-column 15-winding autotransformer

DAMIAN MAZUR, MAREK GOŁĘBIOWSKI

Faculty of Electrical and Computer Engineering,
Rzeszow University of Technology, Rzeszów, Poland
e-mail: mazur@prz.edu.pl

(Received: 02.07.2010, revised: 12.12.2010)

Abstract: The 15-winding and 3-column autotransformer supplying an 18-pulse rectifier circuit was developed. Presented methods can be used also for the autotransformers of other topologies supplying different kinds of converters. Presented methods make it possible to exactly calculate main and leakage inductances of the multi-winding autotransformer. The presented analysis of the eigenvalues and eigenvectors of the inductance matrix makes it possible to identify the influence nature of individual modes on the inductance matrix, and to compare the calculation results obtained using the presented methods. Frequency dependence of autotransformer parameters was shown. Also modes of the impedance matrix of the multi-winding autotransformer was investigated, this made it possible to identify the influence nature of individual modes on the inductance matrix. Using presented methods one can exactly calculate main and leakage inductances of the autotransformer. Thanks to this, one can design in optimal way autotransformers for supplying, for example, rectifier circuits, THD coefficients. The results of the measurements and simulations were also shortly presented at the end of the article.

Key words: autotransformer, leakage inductance, eddy current losses, proximity effect

1. Introduction

Impedance matrix of the autotransformer was calculated with the use of the 3D finite elements method at mono-harmonic voltage supply [1-3]. Eddy current losses in winding copper as well as in core iron were taken into account, what made it possible to study leakage inductances versus pulsation. Mono-harmonic calculations were performed assuming linearity of the magnetic core.

2. Impedance matrix of the autotransformer at the mono-harmonic voltage supply

For the assumed vector of winding supply voltages, the corresponding winding current vector was calculated, and the results were placed in relevant columns of $[U]$ and $[I]$ matrices:

$$[I] = [Z]^{-1} \cdot [U]$$
$$\begin{cases} [Z] = [U] \cdot [I]^{-1} \\ [Z] = [W] \cdot [D] \cdot [W]^{t} \end{cases}, \tag{1}$$

where: $[Z]$ – impedance matrix of the autotransformer; $[W]$, $[D]$ – eigenvectors and eigenvalues of matrix $[Z]$

In the presented method the inverse matrix of $[Z]$ is calculated. Therefore small leakage inductances are calculated more accurately due to numerical reasons.

It is impossible to create the FEM model which could consider in a direct way the magnetic core lamination, because of the practical reasons. However, eddy current losses can be considered in mono-harmonic analysis by introducing complex tensor of the magnetic permeability $\hat{\hat{\mu}}$ and electric conductivity $\hat{\hat{\gamma}}$. Figure 1 is the base of introduction of those parameters for core sheets.

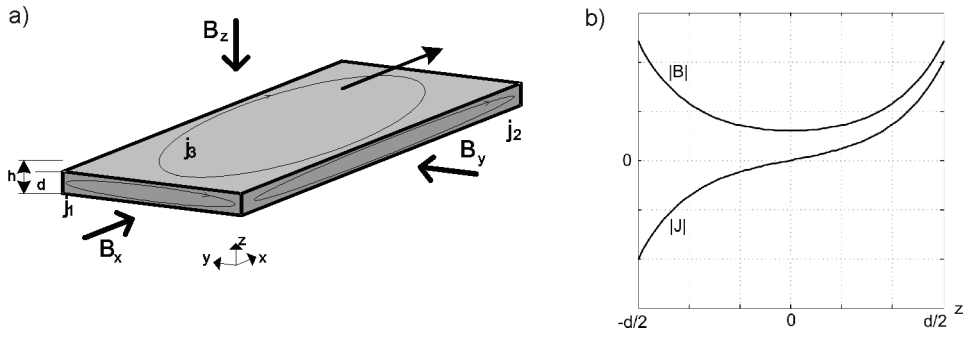

Fig. 1. a) The magnetic core sheet with eddy currents, b) magnetic flux and eddy current density in the core sheet (direction z)

Magnetic permeability $\hat{\hat{\mu}}$ and electric conductivity $\hat{\hat{\gamma}}$ tensors are shown in formulas:

$$\hat{\hat{\mu}} = \begin{pmatrix} k_{fe} \cdot \hat{\mu}_x & 0 & 0 \\ 0 & k_{fe} \cdot \hat{\mu}_y & 0 \\ 0 & 0 & \mu_{zz} \end{pmatrix} \quad \hat{\hat{\gamma}} = \begin{pmatrix} k_{fe} \cdot \gamma & 0 & 0 \\ 0 & k_{fe} \cdot \gamma & 0 \\ 0 & 0 & 0 \end{pmatrix}, \tag{2}$$

where:

$$\delta = \sqrt{\frac{2}{\omega \mu \gamma}}, \quad \hat{\mu} = \mu \frac{\tanh\left[(1+j) \cdot \frac{d}{2\delta}\right]}{(1+j) \cdot \frac{d}{2\delta}}, \quad k_{fe} = \frac{d}{h}. \tag{3}$$

Considering the structure the core sheet, the magnetic complex permeability $\hat{\mu}$ from the formula (3) was responsible for eddy currents in x, y directions from figure 1a. In z direction, the eddy current was the result of electric conductivity in x, y directions in electric conducti-

vity tensor $\hat{\vec{\gamma}}$ from formula (2). Considering the structure of winding area, only the magnetic permeability tensor $\hat{\vec{\mu}}$ was taken into account.

The following system of equations was solved in FEM 3D calculations:

$$\begin{cases} \mathrm{rot}\left((\vec{\mu})^{-1}\ \mathrm{rot}\,\vec{A}\right) = \vec{\gamma}\left(-\dfrac{d\vec{A}}{dt} + grad\left(\dfrac{d}{dt}(\varphi)\right)\right) + \vec{J} = \ldots \\ = \vec{\gamma}\left(-\dfrac{d\vec{A}}{dt} + grad\left(\dfrac{d}{dt}(\varphi)\right)\right) + \sum_{i=1}^{il\_faz}\left(q_i^o \cdot \mathrm{rot}\,\vec{T}_{oi}\right) \\ div\left(\vec{\gamma}\left(-\dfrac{d\vec{A}}{dt} + grad\left(\dfrac{d}{dt}(\varphi)\right)\right)\right) = 0 \\ \dfrac{d}{dt}\psi_j + R_j \cdot q_j^o + L_j\dfrac{di}{dt} = U_j,\ \ (j = 1, 2, \ldots, n) \\ \psi_j = \int_V \left(\mathrm{rot}\left(\vec{T}_{oj}\right)\cdot\vec{A}\right)dV = \int_V \left(\vec{T}_{oj}\cdot\mathrm{rot}\,\vec{A}\right)dV = \int_V \left(\vec{T}_{oj}\cdot\vec{B}\right)dV\,. \end{cases} \tag{4}$$

The third equation is the voltage equation for the windings, where the stream ψ_j was counted in a way given in the last equation. Vector $\vec{J}$ is the winding current density. To identify the position of the winding i the vector $\vec{T}_{oi}$ was introduced, where density of its coils is shown by equation $\mathrm{rot}\,(\vec{T}_{oi})$. In presented method the proximity effect was simulated.

3. Eigenvalues and eigenvectors of inductance matrix [*Z*] of autotransformer versus frequency

Eigenvectors of inductance matrix of the autotransformer show weak variability due to pulsation. Therefore, they can be considered as a spatial transformation matrix between the coordinates of the system: the current flow in autotransformer windings, and coupled fluxes in these windings.

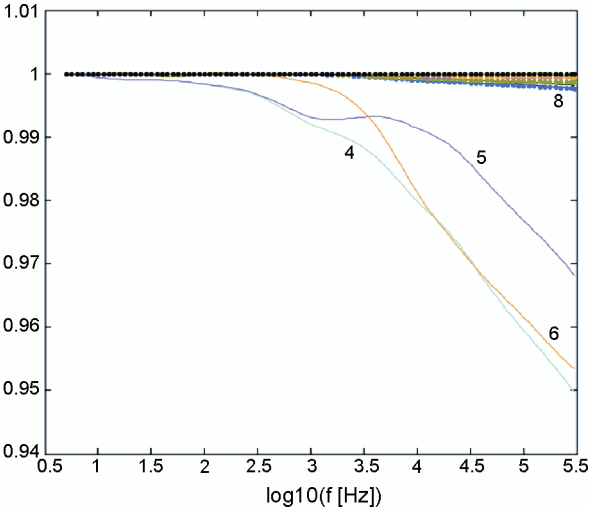

Fig. 2. Scalar products of eigenvectors with vectors computed at lower pulsations – narrow range of variability around 1

First two rows of the Table 1 present the eigenvalues of the impedance matrix (real and imaginary part). Below there are eigenvectors placed in columns, related to these values, respectively. These eigenvectors are divided into six groups. First one (*gł*) consists of two vectors related to the main magnetic flux, the third vector (group *a*) is related to the zero component of the magnetic flux. Following four three-vectors groups (*b*, *c*, *d*, *e*) are related to the leakage magnetic flux. Vectors in these groups are characterized by similar acting and close values of eigenvalues related to them. Vectors from group *b* acts similarly on each magnetic column and thus is similar in a way to the zero component vector, while vectors from groups *c*, *d* and *e* are concentrated each on one column only.

Table 1. Eigenvalues and corresponding to them eigenvectors (with an accuracy to the factor ±1) of the autotransformer impedance matrix [*Z*], (for frequency lower than 4 kHz), A, B, C are denotations of autotransformer columns

R	1.0396e-2	4.01e-3	4.86e-4	4.722e-5	4.699e-5	3.70e-5	1.24e-5	1.179e-5	1.02e-5	6.19e-6	5.582e-6	3.86e-6	3.792e-6	3.27e-6	1.704e-6
L	6.9412e-5	4.14e-5	1.33e-6	9.754e-8	9.664e-8	8.79e-8	2.66e-8	2.529e-8	2.17e-8	1.31e-8	1.186e-8	8.15e-9	8.043e-9	6.94e-9	3.604e-9
nr ww	1gł	2gł	3*a*	4*b*	5*b*	6*b*	7*c*	8*c*	9*c*	10*d*	11*d*	12*d*	13*e*	14*e*	15*e*
A	0.1824	−0.3159	0.2753	−0.4582	−0.1625	−0.2399	0.4697	−0.0529	0.0231	0.3828	−0.0031	−0.0146	0.3556	0.0002	−0.0001
	0.1826	−0.3162	0.2727	−0.3250	−0.1150	−0.1596	−0.0326	0.0049	−0.0049	−0.3838	0.0046	0.0298	−0.7062	−0.0002	−0.0000
	0.1828	−0.3164	0.2645	−0.0490	−0.0168	0.0020	−0.5923	0.0663	−0.0295	−0.3732	0.0024	−0.0216	0.5459	0.0003	−0.0001
	0.1830	−0.3165	0.2490	0.2939	0.1047	0.1917	−0.3617	0.0330	−0.0040	0.6841	−0.0067	0.0082	−0.2650	−0.0003	0.0002
	0.1830	−0.3162	0.2246	0.5428	0.1915	0.3067	0.5303	−0.0667	0.0347	−0.3141	0.0073	0.0044	0.0709	0.0009	−0.0015
B	−0.3643	−0.0000	0.2830	0.3055	−0.2440	−0.3824	−0.0229	0.0380	0.4894	−0.0045	0.0050	−0.3978	−0.0157	−0.0014	−0.2968
	−0.3647	−0.0000	0.2782	0.2139	−0.1702	−0.2550	−0.0004	−0.0008	−0.0699	0.0028	−0.0036	0.4765	0.0191	0.0021	0.6462
	−0.3651	−0.0000	0.2663	0.0316	−0.0234	−0.0066	0.0258	−0.0442	−0.6101	0.0056	−0.0058	0.2557	0.0096	0.0004	−0.5948
	−0.3653	−0.0000	0.2456	−0.1907	0.1548	0.2819	0.0228	−0.0350	−0.3153	−0.0029	0.0046	−0.6610	−0.0262	−0.0024	0.3572
	−0.3654	−0.0000	0.2149	−0.3528	0.2832	0.4628	−0.0129	0.0266	0.5261	−0.0053	0.0045	0.3327	0.0142	0.0024	−0.1135
C	0.1824	0.3159	0.2755	−0.0030	0.4673	−0.2781	−0.0561	−0.4735	0.0310	−0.0055	−0.3868	−0.0024	−0.0003	0.3426	−0.0001
	0.1826	0.3162	0.2728	−0.0018	0.3308	−0.1859	0.0035	0.0411	−0.0059	0.0042	0.4056	0.0052	0.0008	−0.6942	−0.0000
	0.1828	0.3164	0.2645	0.0006	0.0501	−0.0012	0.0707	0.5956	−0.0394	0.0056	0.3468	−0.0017	−0.0003	0.5589	−0.0002
	0.1829	0.3164	0.2489	0.0036	−0.2970	0.2160	0.0488	0.3491	−0.0100	−0.0078	−0.6806	−0.0026	−0.0003	−0.2861	0.0003
	0.1830	0.3162	0.2244	0.0059	−0.5484	0.3501	−0.0547	−0.5286	0.0438	−0.0007	0.3194	0.0077	0.0012	0.0800	−0.0016

4. Autotransformer equivalent circuit

Autotransformer equivalent circuit using LR ladder networks for modeling frequency dependencies of autotransformer parameters was built. The eddy current losses in the magnetic core were simulated by the windings, placed on each column, shorted through the ladder circuits. The frequency dependence of the autotransformer leakage parameters was also simulated in calculations by means of ladder networks supplied by current system after transformation by frequency invariable eigenvectors matrix. Also the magnetic hysteresis losses were included in simulations [4-6]. Optimization methods were used for calculating the length of the magnetic columns of the ladder network in Figure 4. Figure 5 presents comparison of the fre-

quency dependency of the eigenvalues related to main magnetic flux computed in mono-harmonic calculations with the same eigenvalues calculated from the synthesized equivalent circuit.

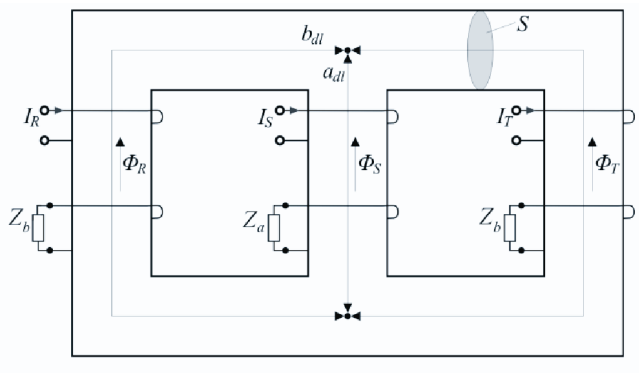

Fig. 3. Three-column equivalent circuit of the autotransformer simulating eddy current losses in the magnetic core by impedances Z_a and Z_b

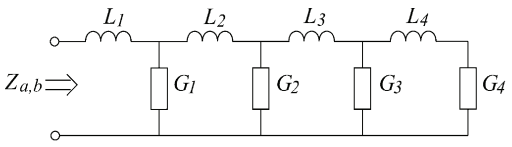

Fig. 4. Cauer's four-segment ladder circuit

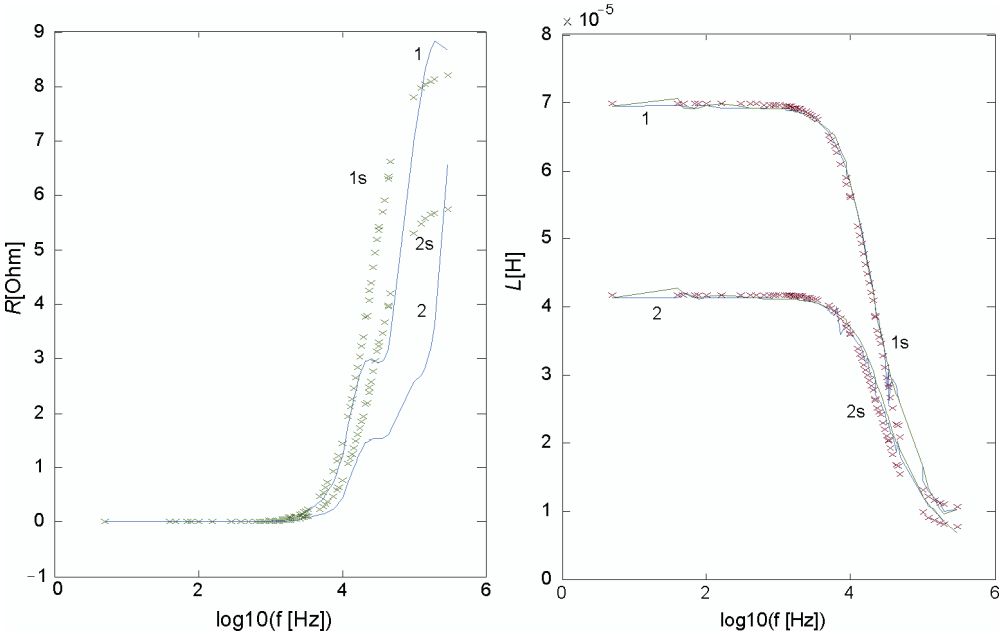

Fig. 5. Eigenvalues (1 and 2 solid line) related to main magnetic flux (real and imaginary parts), calculated from matrix [*Z*] according to formula (1) and from the synthesized equivalent circuit in figure 5 – marked 1s i 2s (dots)

5. Measurement and simulation results

5.1. The arrangement order of the autotransformer windings at the core column

The way of arrangement of the autotransformer windings in the window affects the values of leakage inductances of those windings. The simulation of the examined 18-pulse rectifier circuit was made for the various arrangement orders of the autotransformer windings on the core column. The summary of simulation results is presented in Figures 6 and 7.

As one can see, for various combinations of the windings arrangement, the THD of the converter mains currents was obtained in the range of 4 to 8%, in addition the number of "bad" arrangements is comparable with the number of "good" arrangements. So, the problem of the windings arrangement order appears to be essential. Figure 7 confirms that fact.

The proper order of arrangement of the windings on the autotransformer core can reduce THD coefficient of the converter mains currents.

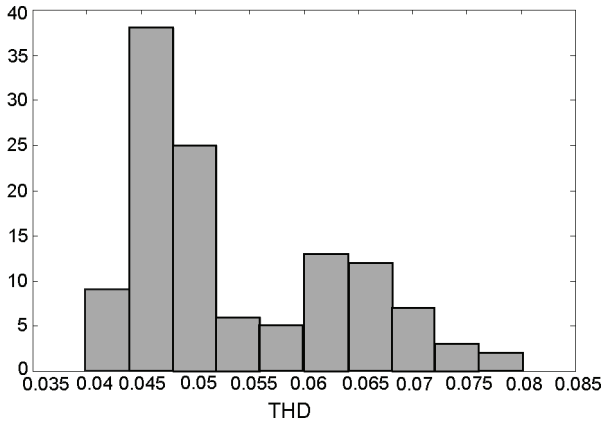

Fig. 6. The histogram of the mains currents THD coefficient obtained for various arrangements of the autotransformer windings and for small inductance of the power grid

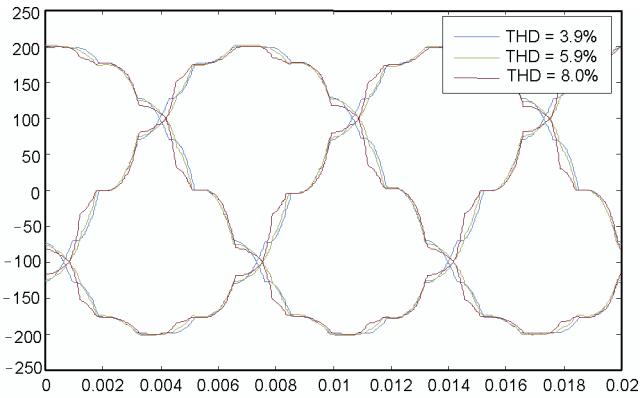

Fig. 7. Mains currents of the converter obtained using leakage inductances calculated for three different orders of arrangement of the windings on the autotransformer

5.2. Experimental model

Developed methods and results were used to design 50 kW autotransformer for 18-pulse rectifier circuit. Figure 8 presents the picture of the autotransformer prototype at the measurement station.

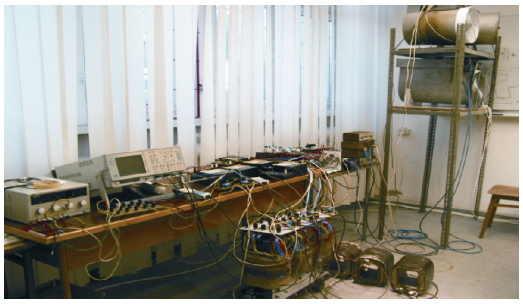

Fig. 8. Autotransformer prototype at the measurement station

A number of simulations were carried out. The eigenvalues numbered 6 and 5 from the Table 1 are worth of notice. Their enlargement makes THD coefficient getting worse even much more than the enlargement of zero component (eigenvalue at number 3). Eigenvectors of these values shows, that in order to suppress them, the windings of the triangle should be placed in outermost places at the core columns.

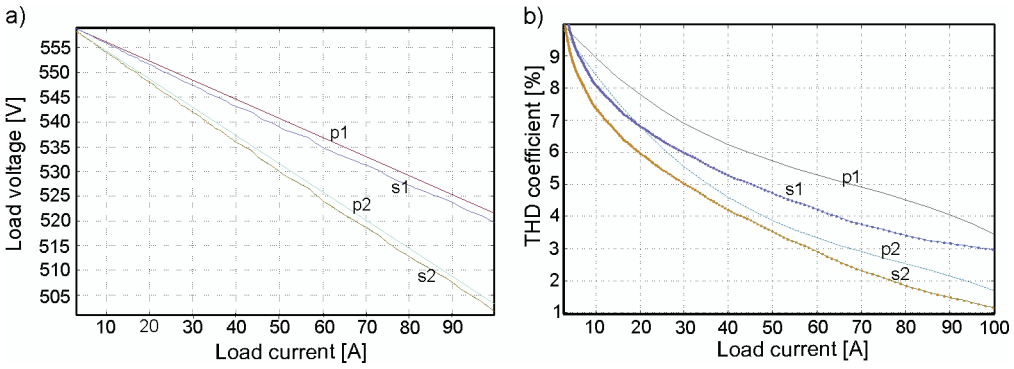

Fig. 9. a) p1 – measurements and s1 – simulations of the load voltage from the load current; similarly p2 and s2 but with additional mains chokes 0.3 mH; b) THD coefficient of the mains currents: p1, s1 – measurements and simulations without mains chokes, p2, s2 with mains chokes 0.3 mH

Figures 9a and 9b present results of the measurements and simulations of the external characteristics and THD coefficient of the mains currents with and without mains chokes 0.3 mH versus load current.

6. Conclusion

The autotransformer leakage inductance calculation methods of different degree of complexity was presented and compared. The zero component related eigenvalue of the leakage in-

ductance matrix is not calculated correctly in 2D methods. However after applying adequate correction, leakage inductances obtained with these methods can be used for converter simulations. The mono-harmonic calculations showed that the leakage inductances of the autotransformer remain constant for frequencies up to 4 kHz. This justifies the use of these inductances obtained in static calculations in the AC/DC converter simulations. The method of equivalent circuit creation of the autotransformer that uses LR ladder networks for modeling frequency dependencies of its parameters was presented.

References

[1] Gołębiowski L., Gołębiowski M., Mazur D., Noga M., *Modelowanie macierzy indukcyjności transformatorów wielouzwojeniowych, trójkolumnowych w funkcji częstotliwości*. XVIII Seminarium Technicznego, KOMEL, Katowice (2009).

[2] Dhomane G.A., Suryawanshi M.H. *Mitigation of harmonics in three-phase ac system using current injection technique for ac-to-dc converter*. Electric Power Systems Research 79: 1374-1383 (2009).

[3] Choi S., Won C.-Y., Kim G.-S. *A New Three-Phase Harmonic-Free Rectification Scheme Based on Zero-Sequence Current Injection*. IEEE Transactions on Industry Applications 41(2): 627-633 (2005).

[4] Villablanca Miguel E., Felipe A. Cruzat et al., *A buck-type low-power rectifier with high-quality waveforms*. Electric Power Systems Research 78: 1899-1905 (2008).

[5] Zakrzewski K. *Overloss coefficient for dynamo sheet during axial magnetization with nonsinusoidal flux*. Archives of Electrical Engineering XLVI(3): 355-365 (1997).

[6] Nan X., Sullivan C.R. *An equivalent complex permeability model for Litz-Wire windings*. IEEE Transactions on Industry Applications 45(2): 854-860 (2009).